JPEDAV (2008) 29:222–230
DOI: 10.1007/s11669-008-9280-5
1547-7037 ©ASM International

Gibbs Energy of Formation of MnO: Measurement and Assessment

K. T. Jacob, A. Kumar, and Y. Waseda

(Submitted August 7, 2006)

Based on the measurements of Alcock and Zador, Grundy et al. estimated an uncertainty of the order of ±5 kJ mol^{-1} for the standard Gibbs energy of formation of MnO in a recent assessment. Since the evaluation of thermodynamic data for the higher oxides Mn_3O_4, Mn_2O_3, and MnO_2 depends on values for MnO, a redetermination of its Gibbs energy of formation was undertaken in the temperature range from 875 to 1300 K using a solid-state electrochemical cell incorporating yttria-doped thoria (YDT) as the solid electrolyte and Fe + $Fe_{1-\delta}O$ as the reference electrode. The cell can be presented as

$$\text{Pt, Mn} + \text{MnO/YDT/Fe} + \text{Fe}_{1-\delta}\text{O, Pt}$$

Since the metals Fe and Mn undergo phase transitions in the temperature range of measurement, the reversible emf of the cell is represented by the three linear segments. Combining the emf with the oxygen potential for the reference electrode, the standard Gibbs energy of formation of MnO from α-Mn and gaseous diatomic oxygen in the temperature range from 875 to 980 K is obtained as:

$$\Delta G_f^o/\text{J mol}^{-1}(\pm 250) = -385624 + 73.071T$$

From 980 to 1300 K the Gibbs energy of formation of MnO from β-Mn and oxygen gas is given by:

$$\Delta G_f^o/\text{J mol}^{-1}(\pm 250) = -387850 + 75.36T$$

The new data are in excellent agreement with the earlier measurements of Alcock and Zador. Grundy et al. incorrectly analyzed the data of Alcock and Zador showing relatively large difference (±5 kJ mol^{-1}) in Gibbs energies of MnO from their two cells with Fe + $Fe_{1-\delta}O$ and Ni + NiO as reference electrodes. Thermodynamic data for MnO is reassessed in the light of the new measurements. A table of refined thermodynamic data for MnO from 298.15 to 2000 K is presented.

Keywords assessment, electromotive force (EMF), experimental thermodynamics, oxide system, thermodynamic properties

1. Introduction

Mixed-valent manganites have been the focus of an intense scientific activity for the past several years in view of the richness of physical phenomenon they display as well as their potential utilization based on their unique physical and chemical properties. The chemical applications include catalysis—they serve as a good catalyst for auto exhausts—and electrochemical engineering, where they are employed as electrodes in oxygen sensors and solid-oxide fuel cells. The catalytic activity is associated with Mn^{3+}-Mn^{4+} mixed valance, and mixed ionic-electronic conductivity is associated with the formation of oxygen vacancies in the solid. Physical properties include the temperature dependence of resistivity and magneto resistance (MR). In these compounds, there is a gigantic decrease of resistance by application of a magnetic field. Such a gigantic negative MR is now termed "colossal magneto resistance" (CMR) to distinguish it from the giant magneto resistance (GMR) observed in transition metal systems in multilayer and granular forms. The potential applications include spin-polarized transport applications, magnetic field sensors, magnetoresistive read-heads, and magnetoresistive random access memory.

Thermodynamic data on manganites is required for evaluating its compatibility with other materials at high temperatures. Thermodynamic data on manganites obtained by either experiment or modeling depend critically on data on the binary and ternary compounds of manganese. Grundy

K. T. Jacob and **A. Kumar**, Department of Materials Engineering, Indian Institute of Science, Bangalore 560 012, India; **Y. Waseda**, Institute for Multidisciplinary Research on Advanced Materials, Tohoku University, Aoba-ku, Sendai 980 8577, Japan. Contact e-mail: katob@materials.iisc.ernet.in.

et al.[1] have recently presented an extensive assessment of the Mn-O system. Using experimental data on thermodynamics properties and phase diagram, a set of model parameters was optimized. They made two important points regarding Gibbs energy of formation of MnO. First, there is only one study by Alcock and Zador[2] using two separate solid-states cells with Fe + $Fe_{1-\delta}O$ and Ni + NiO as reference electrodes. Second, Gibbs energy of formation of MnO derived from the two cells differs significantly. Grundy et al.[1] estimated an uncertainty as the order of ±5 kJ mol^{-1}. Hence they concluded that further measurements of the oxygen potentials for the oxidation of Mn to MnO are highly desirable. In response to this suggestion, new measurements are reported in this article. To minimize the cell emf and consequently errors in measurement, Fe + $Fe_{1-\delta}O$ was chosen as the reference electrode. The oxygen chemical potential associated with this electrode is well established in the literature. In this study, the electrodes were placed under separate flowing streams of prepurified gas at ambient pressure to minimize the volatilization of Mn in contrast to Alcock and Zador[2] who operated their cells in vacuo.

2. Experimental

2.1 Materials

Powders of Fe, Mn, Fe_2O_3, and Mn_2O_3 each of purity greater than 99.99% were used to prepare the electrodes. The oxides were initially heat treated at 1073 K for ~30 ks in dry air. The particle size of the powders were in the range from 2 to 23 μm. Bright green MnO (manganosite) was prepared by reducing Mn_2O_3 contained in a platinum boat in a stream of hydrogen at 1300 K for ~15 ks. Powder X-ray diffraction confirmed the formation of MnO with rock-salt structure with a lattice parameter of 0.4446 nm. In this structure, the large oxygen ions (O^{2-}) are arranged in cubic close packing and all the octahedral interstitial positions are filled with Mn^{2+}. The coordination number is six for both O^{2-} and Mn^{2+}.

The measuring electrode was prepared by mixing Mn and MnO in equimolar ratio, compacting in a steel die at a pressure of 100 MPa and sintering at 1300 K for ~15 ks. The reference electrode was prepared by mixing powders of Fe and Fe_2O_3 in the molar ratio 4:1, compacting into a pellet and sintering at 1373 K in a steam of flowing Ar gas for ~30 ks. After sintering, the pellets consisted of Fe + $Fe_{1-\delta}O$. Although the value of δ in $Fe_{1-\delta}O$ has very small temperature dependence, the mean value is 0.05.

Yttria-doped thoria (YDT) powder was prepared by co-precipitation from an aqueous solution of thorium and yttrium nitrates in the mole ratio 9:1. The nitrate solution with pH controlled at 1.75 was added to a 5 mass % ammonium oxalate solution (pH = 3) at room temperature with vigorous stirring. The precipitate was allowed to settle and then filtered, dried, and ignited at 1173 K to give the oxide solid solution. The solid solution was ground and heated at 1473 K to give a pale brown powder. Methyl methacrylate binder dissolved in toluene was added to the oxide solid solution, stirred and the solvent evaporated under infrared light. The powder was ground and pressed into pellets 15 mm in diameter and 2 mm thick. The binder was removed by heating at 1273 K in air. The pellet was sintered at 2273 K for 3 h in a vacuum furnace. The YDT pellets thus obtained were oxygen deficient. The stoichiometry was restored by heating first in air and then in a gas stream ($P_{H_2}/P_{H_2O} \approx 1$) at 1273 K. The polished YDT pellets were white, dense, and nearly transparent. The flat surfaces of the YDT and electrode pellets were polished with silicon carbide powder of 600 mesh and the cleaned with acetone.

High purity (99.999%) argon gas used in this study was dried by passing over anhydrous silica gel, magnesium perchlorate, and phosphorus pentoxide, and deoxidized by passing through copper wool at 723 K and by titanium sponge at 1123 K prior to use.

2.2 Apparatus

Apparatus used in this study is similar to that described elsewhere.[3] The reference and test electrodes were spring loaded against the two polished surfaces of a YDT-electrolyte pellet by a rig consisting of alumina rings and slabs. The assembly was suspended inside a vertical alumina tube flushed with prepurified Ar gas. The space around the measuring electrode was isolated by a second alumina tube spring loaded against the YDT pellet. The alumina tube surrounding the measuring electrode was also flushed with a separate stream of prepurified Ar gas. With this arrangement the gas atmospheres around the two electrodes were physically separated thus preventing transport of oxygen and manganese between the electrodes via the gas phase.

Because of the very low oxygen partial pressure over the measuring electrode, it was necessary to ensure that the Ar gas flowing over it was well deoxidized. Titanium internal getters were placed in the path of incoming Ar stream at a location approximately 60 mm from the cell were the temperature was ~300 K below that of the cell. The internal getters removed residual oxygen in the Ar and oxygen bearing gas species that desorb gradually from the alumina tubes and supports. The position of the internal getters was adjusted such that the oxygen partial pressure in the Ar gas was of the same order as that prevailing over the electrode.

The electrical contact to the electrodes was made by insulated platinum leads. Insulation was provided by thermal spray coating of alumina. The temperature of the cell was measured by a Pt/Pt-13%Rh thermocouple placed adjacent to the cell within 4 mm. The thermocouple was checked against the melting point of Au. The temperature of the furnace was controlled to ±1 K.

2.3 Procedure

After assembling the cell, the outer alumina tube enclosing the cell was evacuated to a pressure of 10 Pa, and then refilled with prepurified Ar gas. This procedure was repeated after heating the cell to 850 K to remove most of the oxygen bearing gas species that were absorbed on the ceramic tubes. The molecules that desorb at higher temperatures are captured by the internal getters.

After attainment of constant temperature, the cell registered constant emf in 0.6-1.5 ks; longer period was required at lower temperatures. The reversible emf of the cell was measured in the temperature range from 875 to 1300 K at intervals of 25 K using a high impedance (10^{12} Ω) digital voltmeter. The reversibility of the cell was checked by passing small direct current (~10 μA) through the cell for ~0.3 ks in either direction using an external circuit. The current caused polarization of the electrodes and the cell voltage was displaced from the equilibrium value. The open circuit voltage was found to approach the equilibrium value after 0.8-2 ks depending on the temperature of the cell. Since the cell voltage returned to the same value after displacement in opposite directions, reversibility was ascertained. The cell emf was also found to be independent of the flow rate of inert gas over the electrodes and to be reproducible on temperature cycling.

Below 875 K, there was a small drift in emf with time and reversibility and reproducibility were poor. The vapor pressure of Mn set the upper limit of temperature for cell operation.

3. Results

The measured emf of cell I is plotted as a function of temperature in Fig. 1. The emf is nonlinear in the temperature range from 875 to 1300 K. Both metals Fe and Mn present at the electrodes undergo phase transformation in this temperature range. Hence the emf data are analyzed in three temperature ranges; 875-980, 980-1185, and 1185-1300 K. The phase change α → β of Mn occurs at 980 K and α → γ transformation of Fe happens at 1185 K.[4] The least-squares regression analysis gives the following equations for the emf:

$$E_{\mathrm{l}}, \mathrm{V}\ (\pm 0.34) = 634.81 - 0.0460T \qquad (875\text{-}980\ \mathrm{K})$$

$$E_{\mathrm{i}}, \mathrm{V}\ (\pm 0.42) = 646.34 - 0.05781T \qquad (980\text{-}1185\ \mathrm{K})$$

$$E_{\mathrm{h}},\ \mathrm{V}\ (\pm 0.20) = 638.86 - 0.05160T \qquad (1185\text{-}1300\ \mathrm{K})$$

where the uncertainty limit corresponds to twice the standard deviation. Systematic errors from the various sources are estimated as ±0.4 mV. The emfs E_{l} and E_{i} for the low and intermediate temperature ranges intersect at 976 K close to phase transformation temperature for Mn (980 K).[4] The emfs E_{i} and E_{h} for the intermediate and high-temperature ranges intersect at 1204 K, a little higher than the α → γ transformation temperature for Fe (1185 K).[4] Considering the small changes in slope at phase transformation temperatures, limited temperature range for emf measurement in each segment and the uncertainty in emf, the difference of 19 K is not considered to be serious.

The oxygen potentials at the two electrodes fall within the electrolytic conduction domain ($t_{\mathrm{ion}} > 0.99$) of YDT electrolyte.[5] The oxygen potential of the measuring electrode is below the lower limit for fully ionic conduction in stabilized-zirconia electrolytes. Hence the choice of YDT is made. The emf is related to the difference in oxygen potentials at the two electrodes by the Nernst equation: $\Delta\mu_{O_2} = nFE$. Combining the emf with the oxygen chemical potential of the $Fe + Fe_{1-\delta}O$ reference electrode,[6] the Gibbs energy of formation of MnO with rock salt (rs) structure can be calculated as function of temperature. MnO in equilibrium with Mn is essentially stoichiometric.[7,8]

For the reaction,

$$\mathrm{Mn}\ (\alpha) + 1/2\mathrm{O_2}\ (\mathrm{g}) \rightarrow \mathrm{MnO}\ (\mathrm{rs})$$

$$\Delta G^{\mathrm{o}}_{\mathrm{f}},\ \mathrm{J\,mol^{-1}}\ (\pm 250) = -385624 + 73.071T$$

in the temperature range from 875 to 980 K. The uncertainty in the oxygen chemical potential of reference electrode is incorporated in the total error estimate given. For the reaction,

$$\mathrm{Mn}\ (\beta) + 1/2\mathrm{O_2}\ (\mathrm{g}) \rightarrow \mathrm{MnO}\ (\mathrm{rs})$$

$$\Delta G^{\mathrm{o}}_{\mathrm{f}},\ \mathrm{J\,mol^{-1}}\ (\pm 250) = -387849 + 75.348T\ (980\text{-}1185\ \mathrm{K})$$

$$\Delta G^{\mathrm{o}}_{\mathrm{f}},\ \mathrm{J\,mol^{-1}}\ (\pm 250) = -387853 + 75.371T\ (1185\text{-}1300\ \mathrm{K})$$

The equations obtained from the two different temperature ranges are very similar and an average value of $\Delta G^{\mathrm{o}}_{\mathrm{f}}$ for the formation of MnO from β-Mn and diatomic oxygen

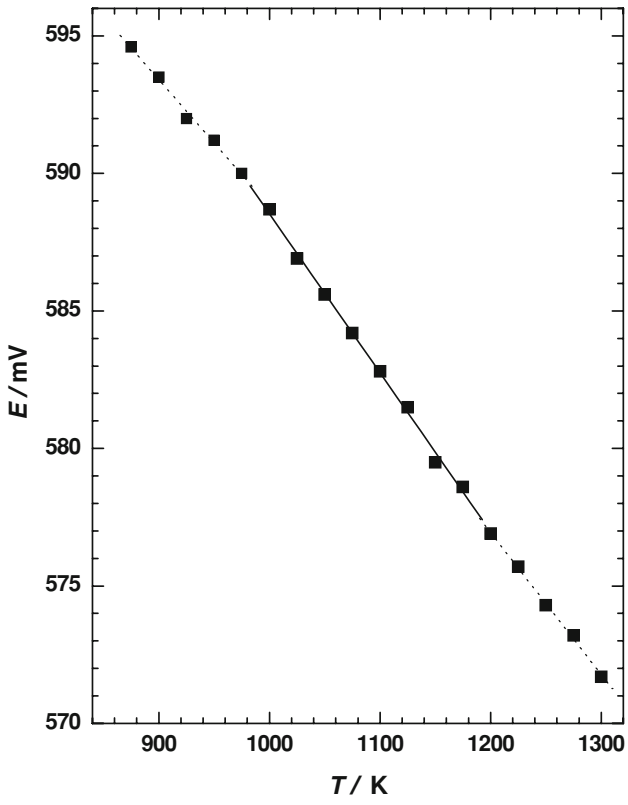

Fig. 1 Variation of the emf of the electrochemical cell as a function of temperature

gas (rounded off to 10 J/mol) is chosen for the temperature range from 980 to 1300 K;

$$\Delta G_f^o, \text{J mol}^{-1}\ (\pm 250) = -387850 + 75.36T$$

Following the second law of thermodynamics, the temperature independent term in this equation can be viewed as the average value for the enthalpy of formation of MnO in the temperature range or the enthalpy of formation at a mean temperature (1140 K). The temperature dependent term is related to the entropy of formation at the mean temperature.

The values obtained in this study are compared with those obtained from the measurements of Alcock and Zador[2] in Table 1. Alcock and Zador[2] measured the Gibbs energy of formation of MnO using solid-state cells with Ni + NiO and Fe + $Fe_{1-\delta}O$ reference electrodes. They combined the results on Gibbs energy of formation of MnO from both cells and represented their combined results by a single equation. They used thermodynamic data for the reference electrodes NiO and $Fe_{1-\delta}O$ from Steele.[9] More precise data for NiO and $Fe_{1-\delta}O$ are now available. Hence the emf data of Alcock and Zador[2] have been reanalyzed using the new data for NiO and $Fe_{1-\delta}O$. Since it was difficult to read exactly the values of emf from the graph in the article, the actual emf values were obtained from Tables 3.2 and 3.3 of the Ph.D. thesis of Zador.[10] The scatter in the emf with Fe + $Fe_{1-\delta}O$ reference electrode was ±1.9 mV; with Ni + NiO reference electrode the scatter was larger (±2.5 mV). They did not observe any change in slope of the emf as a function of temperature in the range 923-1273 K.

Data for each cell is analyzed separately using the Gibbs energy of formation of NiO reported by O'Neill and Pownceby[11] and $Fe_{1-\delta}O$ from the assessment of Sundman.[6]

$$\text{Ni} + 1/2O_2 \rightarrow \text{NiO}$$

$$\Delta G^o, \text{J mol}^{-1} = -239484 + 124.202T - 4.898T \ln T\ (700\text{-}1700\,\text{K})$$

Table 1 Comparison of the measured Gibbs energies of formation of MnO

	ΔG^o, J mol^{-1}		
T, K	This study (Fe + $Fe_{1-\delta}O$ ref)	Alcock and Zador (Fe + $Fe_{1-\delta}O$ ref) (a)	Alcock and Zador (Ni + NiO ref) (a)
900	−319,860	−319,801	−320,273
980	−313,997	−313,777	−314,059
1000	−312,490	−312,271	−312,506
1100	−304,954	−304,741	−304,739
1200	−297,418	−297,211	−296,972
1300	−289,882	−289,681	−289,205

(a) Recalculated from their emfs using more recent data on the reference electrodes

$$(1-\delta)\ \text{Fe (bcc)} + 1/2O_2 \rightarrow Fe_{1-\delta}O$$

$$\Delta G^o, \text{J mol}^{-1} = -263125 + 64.192T\ (800\text{-}1185\,\text{K})$$

$$(1-\delta)\ \text{Fe (fcc)} + 1/2O_2 \rightarrow Fe_{1-\delta}O$$

$$\Delta G^o, \text{J mol}^{-1} = -264573 + 65.414T\ (1185\text{-}1400\,\text{K})$$

The recalculated Gibbs energy of formation of MnO from the emf measurements of Alcock and Zador[2] in the temperature range from 923 to 1273 K can be expressed by two linear equations, one for each cell;

$$\Delta G_{MnO}^o, \text{J mol}^{-1} = -387571 + 75.30T\ (\pm 380)\quad (\text{Fe} + Fe_{1-\delta}O \text{ reference})$$

$$\Delta G_{MnO}^o, \text{J mol}^{-1} = -390176 + 77.67T\ (\pm 480)\quad (\text{Ni} + \text{NiO reference})$$

The recalculated data are very close to the original values suggested by Alcock and Zador.[2] The comparison in Table 1 indicates that the results of this study essentially refine the values reported by Alcock and Zador. Both sets of data, especially from conceptually identical cells with Fe + $Fe_{1-\delta}O$ reference electrode, are in good agreement. Alcock and Zador[2]operated their cells in vacuo. Small but continuous volatilization of Mn from the measuring electrode may be the reason for the small difference in emf between the two studies and the larger scatter in their emf results. Table 1 clearly shows the analysis of Grundy et al.[1] of the emf measurements of Alcock and Zador[2] and their assessment of uncertainty on the Gibbs energy of formation of MnO are incorrect.

4. Discussion

The third-law of thermodynamics provides a better method for deriving the enthalpy of formation from measurement of the corresponding Gibbs energy at high temperatures. It allows the calculation of the formation enthalpy from each data point. If the same value is obtained for enthalpy of formation at a reference temperature from Gibbs energy of formation at different temperatures, then internal consistency of all data used is confirmed. The third-law method is based on knowledge of the absolute entropy of the reactants and products based on low-temperature heat capacity measurements and the third law. To assess the best value for the entropy of MnO, an assessment of the available heat capacity data is required.

4.1 Low-Temperature Heat Capacity and Entropy at 298.15 K

Displayed in Fig. 2 are heat capacities of MnO from 0 to 400 K reported by different investigators. Although there is good general agreement, there are differences in detail. In the temperature range of 225-300 K heat capacity reported

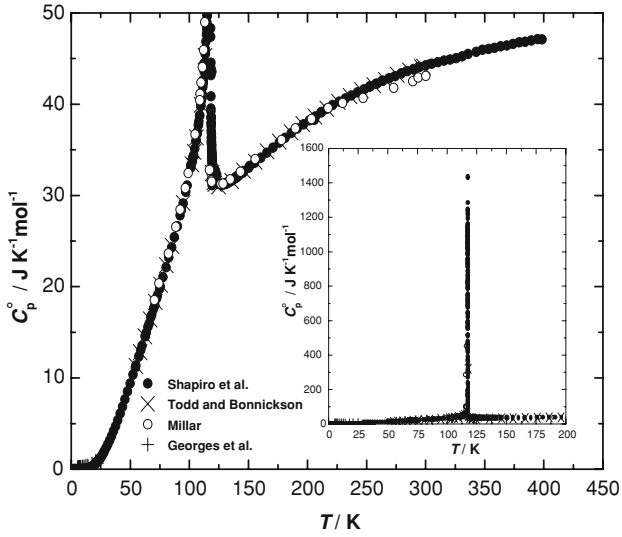

Fig. 2 Comparison of low-temperature (0-400 K) heat capacities reported by Millar,[12] Todd and Bonnickson,[13] Georges et al.,[15] and Shapiro et al.[14]

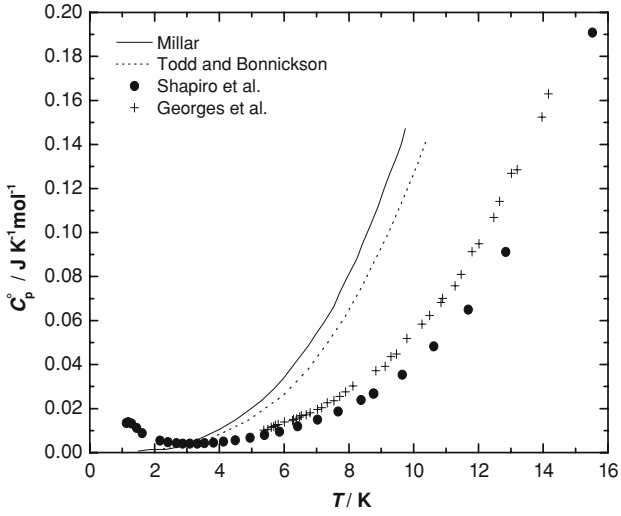

Fig. 3 Comparison of the measured data of Georges et al.[15] and Shapiro et al.[14] close to absolute zero with extrapolated data of Millar[12] and Todd and Bonnickson[13]

by Millar[12] is slightly lower than those of Todd and Bonnickson[13] and Shapiro et al.[14] The transition from antiferromagnetic to paramagnetic state occurs at Neel temperature T_N = 117.7 K.[9]

Millar[12] measured the heat capacity of MnO in the temperature range from 70 to 300 K. To calculate the entropy at 298.15 K, a large extrapolation to 0 K is required. Data above the transition were used to determine the Debye and Einstein coefficients. Millar[12] calculated a value of 62.4 J K^{-1} mol^{-1} for entropy of MnO at 298.15 K. The uncertainty in entropy at 298.15 K is estimated as ±1.4 J K^{-1} mol^{-1}. Todd and Bonnickson[13] measured the heat capacity of MnO using an adiabatic calorimeter in the temperature range from 52 to 298.15 K and calculated entropy of MnO at 298.15 K as 59.71, quoting an uncertainty of ±0.42 J K^{-1} mol^{-1}. They used their lowest temperature data to determine the Debye and Einstein coefficients. In view of uncertainty in extrapolation of heat capacity at low temperatures, the real uncertainty is probably ±1 J K^{-1} mol^{-1}. Georges et al.[15] measured heat capacity from 4 to 40 K. As shown in Fig. 3, their measured heat capacity was substantially lower than the extrapolated data of Millar,[12] and Todd and Bonnickson.[13] Shapiro et al.[14] measured the heat capacity of MnO in the temperature range from 1 to 400 K using different types of experimental techniques: an adiabatic calorimeter from 63 to 298 K and a semi-adiabatic pulse technique from 1 to 10 K. An isothermal technique was used for 10 to 75 K. Their heat capacity at low temperatures is lower than that reported by Georges et al.[15] Shapiro et al.[14] calculated a value 59.02 J K^{-1} mol^{-1} for entropy of MnO at 298.15 K. An error estimate was not given by Shapiro et al.,[14] but can be estimated as (±0.4 J K^{-1} mol^{-1}) in view of the anomalous behavior for $T < 3$ K, which was ignored in the assessment of entropy.

The transition temperature, heat capacity at transition temperature, transition entropy and entropy at 298.15 K reported by different investigations are compared in Table 2. Also listed is the theoretical transition entropy calculated using the relation $\Delta S_{tr}^{o} = R\ln(\beta + 1)$, where $\beta = 5$ is number of unpaired electrons associated with Mn^{2+}. The entropy of transition suggested by Shapiro et al.[14] is closer to theoretical value than those reported by Millar[12] and Todd and Bonnickson.[13] Improved instrumentation allowed Shapiro et al.[14] to determine heat capacity at very small increments in temperature (~0.02 K) so that the peak could be resolved with greater precision.

Table 2 Comparison of heat capacity at transition temperature, transition entropy, and the standard entropy at 298.15 K of MnO

Source	Transition temperature, K	Heat capacity at the transition temperature, J K^{-1} mol^{-1}	Transition entropy ΔS_{tr}^{o}, J K^{-1} mol^{-1}	$S_{298.15}^{o}$, J K^{-1} mol^{-1}
Millar[12]	115.9	450.03	3.88	62.4
Todd and Bonnickson[13]	117.7	320.9	2.72	59.71
Shapiro et al.[14]	117.7	1429.1	12.14	59.02
Theoretical	...	...	14.9	...

Given the large difference in the heat capacities shown in Fig. 3, at first sight it is surprising that the standard entropy at 298.15 K suggested by Todd and Bonnickson[13] and Shapiro et al.[14] are so close. The higher low-temperature heat capacity of Todd and Bonnickson[13] is compensated by their low value at the transition temperature. The low value for transition entropy suggested by Todd and Bonnickson,[13] compensate the higher entropy contribution obtained by integrating their low temperature extrapolated heat capacity. The standard entropy of MnO at 298.15 K is

selected as 59.02 J K^{-1} mol^{-1} essentially based on the most recent higher precision measurements of Shapiro et al.[14]

4.2 High-Temperature Heat Content and Heat Capacity of MnO

Southard and Shomate[16] reported high-temperature heat content $(H^{o}_{T} - H^{o}_{298.15})$ of MnO in the temperature range from 519 to 1773 K by drop calorimetry. Samples of MnO were dropped from a platinum-rhodium high-temperature furnace into a copper block calorimeter. The heat content was found to vary continuously with temperature with no evidence of phase change. The data were fitted by a nonlinear least-squares procedure to obtain an expression for heat content, differentiation of which gave values for heat capacity in the temperature range from 519 to 1773 K. Values thus obtained are compared in Fig. 4 with heat capacity data measured by Shapiro et al.[14] in the temperature range from 298.15 to 400 K. There is reasonable agreement between the low and high temperature heat capacity data. Both sets of data were fitted by the nonlinear least squares procedure to obtain an expression for the heat capacity for MnO in the temperature range from 298.15 to 1800 K:

$$C^{o}_{p}, \mathrm{J\,K^{-1}\,mol^{-1}} = 56.405 + 0.00543T - 236.922T^{-1/2}$$

The fitted curve is in good accord with experiment information as illustrated in Fig. 4. From this equation reassessed values for $(H^{o}_{T} - H^{o}_{298.15})$ and $(S^{o}_{T} - S^{o}_{298.15})$ for MnO are calculated.

4.3 Enthalpy of Formation of MnO at 298.15 K

The third-law analysis of the high-temperature data on Gibbs energy of formation of MnO is based on the equation,

$$\Delta_f H^{o}_{298.15} = \Delta_f G^{o}(T) - \Delta(H^{o}_{T} - H^{o}_{298.15}) + T\{\Delta_f S^{o}_{298.15} + \Delta(S^{o}_{T} - S^{o}_{298.15})\}$$

where $(H^{o}_{T} - H^{o}_{298.15})$ for each phase can be calculated as $\int_{298.15}^{T} C^{o}_{p}\,dT$ and $(S^{o}_{T} - S^{o}_{298.15})$ can be calculated as $\int_{298.15}^{T} (C^{o}_{p}/T)\,dT$. The quantity $\Delta(H^{o}_{T} - H^{o}_{298.15})$ represents the difference of $\sum (H^{o}_{T} - H^{o}_{298.15})$ between products and reactants.

For assessing the entropy of formation of MnO at 298.15 K $(\Delta_f S^{o}_{298.15})$ and values of $\Delta(H^{o}_{T} - H^{o}_{298.15})$ and $\Delta(S^{o}_{T} - S^{o}_{298.15})$, auxiliary data on O_2 gas and Mn metal are also needed. High-temperature heat content $(H^{o}_{T} - H^{o}_{298.15})$, entropy increment $(S^{o}_{T} - S^{o}_{298.15})$ and standard entropy $\{S^{o}_{298.15}, \mathrm{J\,K^{-1}\,mol^{-1}} = 32.221\ (\pm 0.1)\}$ of Mn metal were taken from Desai[17] and the corresponding quantities for O_2 gas from JANAF thermochemical tables[18] $\{S^{o}_{298.15}, \mathrm{J\,K^{-1}\,mol^{-1}} = 205.147\ (\pm 0.035)\}$. Using the selected standard entropy of MnO at 298.15 {59.02 (±0.3) J K^{-1} mol^{-1}}, the standard entropy of formation $\Delta S^{o}_{298.15}$ is –75.78 J K^{-1} mol^{-1}. Third-law analysis of all the high temperature data on Gibbs energy of formation of MnO was carried out. Three sets of data were analyzed: two sets from Alcock and Zador,[2] with Fe + $Fe_{1-\delta}O$ and Ni + NiO as reference electrodes, and one set from this study. Values of $\Delta H^{o}_{298.15}$ were calculated from each value of the Gibbs energy change at high temperatures. The results are plotted as a function of the temperature of Gibbs energy measurement in Fig. 5. The error limits shown for $\Delta H^{o}_{298.15}$ from third-law analysis are approximately the same as that for the Gibbs energy of formation. The purpose of error bars is to see if the variation in $\Delta H^{o}_{298.15}$ with temperature is with in the uncertainty of the Gibbs energy data. High-temperature emf data of Alcock and Zador[2] with Ni + NiO reference

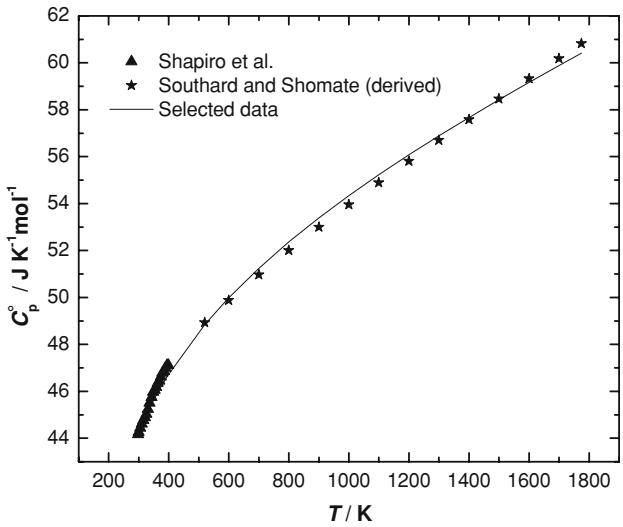

Fig. 4 High-temperature heat capacity of MnO in the range from 298.15 to 1800 K—comparison of selected data with direct (Shapiro et al.[14]) and indirect (Southard and Shomate[16]) experimental information

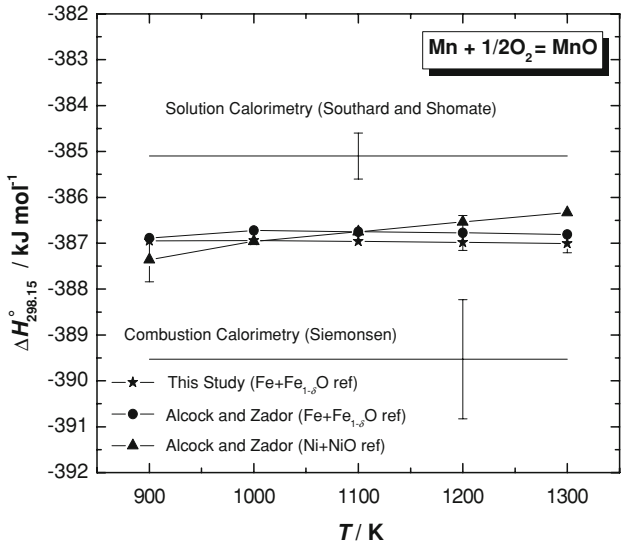

Fig. 5 Results of "third-law" analysis of Gibbs energy of formation of MnO in comparison with direct calorimetric data on enthalpy of formation (Southard and Shomate[16] and Siemonsen[19])

electrode shows systematic increase of $\Delta H^{o}_{298.15}$ with temperature, although the variation is only slightly larger than the error limit of Gibbs energy data. Their data obtained using Fe + $Fe_{1-\delta}O$ as reference electrode shows reasonably constant value for $\Delta H^{o}_{298.15}$. The Gibbs energy of formation obtained in this study also generates a reasonably constant value of $\Delta H^{o}_{298.15}$, which is slightly lower (~225 J mol^{-1}) than that from Alcock and Zador[2] using the same reference electrode.

The calorimetric information on enthalpy of formation at 298.15 K is also shown in Fig. 5 for comparison. Siemonsen[19] measured the enthalpy of formation of

Table 3 Comparison of selected data for MnO with values in the literature

	$\Delta H^{o}_{298.15}$, kJ mol^{-1}		$S^{o}_{298.15}$, J K^{-1} mol^{-1}	
Source	Value	Method	Value	Method
Siemonsen[19]	–389.53 (±1.3)	Combustion calorimetry	...	...
Southard and Shomate[16]	–385.10 (±0.5)	Solution calorimetry	...	...
Millar[12]	...	...	62.4 (±1.4)	Heat capacity 70-300 K
Todd and Bonnickson[13]	...	...	59.71 (±1.0)	Heat capacity 55-298 K
Shapiro et al.[14]	...	...	59.02 (±0.4)	Heat capacity 1-400 K
Robie and Hemingway[20]	–385.22	Assessment	...	...
Wagman et al.[21]	–385.22	Compilation	59.706	Compilation
Knacke et al.[22]	–382.54	Compilation	58.994	Compilation
Pankratz[4]	–385.22	Compilation	59.706	Compilation
Grundy et al.[1]	–386.74 (±5)	Optimization	59.02	Heat capacity/optimization
This study	–386.968 (±0.5)	Third law analysis	59.02 (±0.4)	Selected

Table 4 Reassessed thermodynamic data for MnO

T, K	C^{o}_{p}, J K^{-1} mol^{-1}	$H^{o} - H^{o}_{298.15}$, J mol^{-1}	S^{o}, J K^{-1} mol^{-1}	$-(G^{o} - H^{o}_{298.15})/T$, J K^{-1} mol^{-1}	ΔH^{o}_{f}, kJ mol^{-1}	ΔG^{o}_{f}, kJ mol^{-1}
298.15	44.30	0	59.02	59.02	–386.968	–364.376
300	44.36	82	59.29	59.02	–386.962	–364.236
400	46.73	4643	72.40	60.79	–386.622	–356.711
500	48.52	9409	83.03	64.21	–386.322	–349.270
600	49.99	14337	92.01	68.11	–386.087	–341.883
700	51.25	19400	99.81	72.10	–385.920	–334.530
800	52.37	24583	106.73	76.00	–385.818	–327.196
900	53.39	29872	112.96	79.77	–385.774	–319.873
980	54.16	34174	117.54	82.66	–385.769	–314.045
980	54.16	34174	117.54	82.66	–387.994	–314.046
1000	54.34	35259	118.63	83.37	–388.016	–312.506
1100	55.23	40738	123.85	86.82	–388.080	–304.951
1200	56.08	46305	128.70	90.11	–388.120	–297.393
1300	56.89	51954	133.22	93.25	–388.136	–289.830
1360	57.37	55381	135.80	95.07	–388.136	–285.326
1360	57.37	55381	135.80	95.07	–390.256	–285.326
1400	57.67	57682	137.46	96.26	–390.400	–282.205
1411	57.76	58317	137.91	96.58	–390.455	–281.361
1411	57.76	58317	137.91	96.58	–392.335	–281.362
1500	58.43	63488	141.47	99.14	–392.836	–274.338
1519	58.57	64599	142.20	99.68	–392.971	–272.882
1519	58.57	64599	142.20	99.68	–403.971	–272.881
1600	59.17	69368	145.26	101.91	–404.393	–265.834
1700	59.89	75321	148.87	104.56	–404.890	–257.159
1800	60.59	81345	152.31	107.12	–405.327	–248.456
1900	61.29	87440	155.61	109.59	–405.706	–239.730
2000	61.97	93602	158.77	111.97	–406.028	–230.985

MnO at 298.15 K as −389.53 (±1.3) kJ mol^{-1} using combustion calorimetry. The combustion of manganese metal with oxygen in the bomb calorimeter yields a mixture of oxides MnO and Mn_3O_4. The oxide mixture consists of 10-50% MnO. Large errors in the heat of formation so obtained may result from rather minor error in the analysis of the resulting mixture. Therefore, the enthalpy of formation of MnO was based on the combustion of MnO to Mn_3O_4. This requires the use of paraffin oil as promoter and also yields mixed product requiring some corrections. Southard and Shomate[16] measured the heat of formation of MnO at 298.15 K as −385.10 (±0.5) kJ mol^{-1} by solution calorimetry using 1.006 N sulfuric acid as the solvent. The limits of error were estimated as the sum of the average deviations from the mean of the heats of solution of Mn and MnO, plus 0.05% of the total energy measured, plus 10% of the correction for vaporization of water, plus ±38 J uncertainty in the enthalpy of formation of water.

The value from combustion calorimetry by Siemonsen[19] is significantly more negative and that from solution calorimetry of Southard and Shomate[16] significantly more positive than values obtained from the third-law analysis. The results of the third-law analysis fall between those from combustion and solution calorimetry, but well outside the error limits of the calorimetric measurements. In view of these considerations, the value obtained by third-law analysis of the results of this study on MnO $\Delta H^{o}_{298.15}$, kJ mol^{-1} = −386.968 (±0.5) was selected. The uncertainty estimate is based on errors in all input data, Gibbs energy, entropy, and heat capacity.

Comparison of selected data $\Delta H^{o}_{298.15}$ and $\Delta S^{o}_{298.15}$ for MnO with values available in the literature is presented in Table 3. The literature values are taken from calorimetric measurements, assessments or compilations. Based on the basic thermodynamic data for MnO evaluated in this study, a table of refined data for MnO is prepared (Table 4). Thermodynamic properties are listed at regular intervals of temperature and at temperatures of all phase transitions. Values given in this table supersede those available in earlier compilations and assessments.

5. Conclusions

Analysis of the emf results of Alcock and Zador[2] by Grundy et al.[1] is misleading. The results from the two cells used by Alcock and Zador are quite consistent. The new measurements of higher precision reported in this study provide confirmation of earlier data of Alcock and Zador.[2] Based on the new results and other information in the literature, an internally consistent set of refined thermodynamic data for MnO from 298.15 to 2000 K is presented. The uncertainty in enthalpy of formation of MnO at 298.15 K is ±0.5 kJ mol^{-1} in contrast to ±5 kJ mol^{-1} suggested by Grundy et al.[1] The refined thermodynamic data presented in the temperature range from 298.15 to 2000 K supersede those available in current compilations and assessments.

References

1. A.N. Grundy, B. Hallstedt, and L.J. Gauckler, Assessment of the Mn-O System, *J. Phase Equilibria*, 2003, **24**, p 21-39
2. C.B. Alcock and S. Zador, Thermodynamic Study of Manganese/Manganous-Oxide System by the Use of Solid Oxide Electrolytes, *Electrochim. Acta*, 1967, **12**, p 673-677
3. K.T. Jacob, Potentiometric Determination of the Gibbs Free Energy of Formation of Cadmium and Magnesium Chromites, *J. Electrochem. Soc.*, 1977, **124**, p 1827-1831
4. L.B. Pankratz, Thermodynamic Properties of Elements and Oxides, *Bull. U.S. Bur. Mines*, 1982, **672**, p 229-236
5. J.W. Patterson, Conduction Domains for Solid Electrolytes, *J. Electrochem. Soc.*, 1971, **118**, p 1033-1039
6. B. Sundman, An Assessment of the Fe-O System, *J. Phase Equilibria*, 1991, **12**, p 127-140
7. M.W. Davies and F.D. Richardson, The Non-Stoichiometry of Manganous Oxide, *J. Chem. Soc. Faraday Trans.*, 1959, **55**, p 604-610
8. P. Kofstad, Defects and Diffusion in MnO, *J. Phys. Chem. Solid*, 1983, **44**, p 879-889
9. B.C.H. Steele, High Temperature Thermodynamic Measurements Involving Solid Electrolyte Systems, *Electromotive Force Measurements in High Temperature Systems*, C.B. Alcock, Ed., (London), Institution of Mining and Metallurgy, 1968, p 3-27
10. S. Zador, "Thermodynamic Studies of Non-Stoichiometry in Oxides with Rutile Structure," Ph.D. Thesis, University of London, U.K., 1967
11. H.S. O'Neill and M.I. Pownceby, Thermodynamic Data from the Redox Reactions at High Temperature. I. An Experimental and Theoretical Assessment of the Electrochemical Method Using Stabilized Zirconia Electrolytes, With Revised Values for the Fe-'FeO', Co-CoO, Ni-NiO, Cu-Cu_2O Oxygen Buffers and New Data for the W-WO_2 Buffer, *Contrib. Mineral. Petrol.*, 1993, **114**(3), p 296-314
12. R.W. Millar, The Specific Heats at Low Temperatures of Manganous Oxide, Manganous-Manganic Oxide and Manganese Dioxide, *J. Am. Chem. Soc.*, 1928, **50**, p 1875-1883
13. S.S. Todd and K.R. Bonnickson, Low-Temperature Heat Capacities and Entropies at 298.15 K of Ferrous Oxide, Manganous Oxide and Vanadium Monoxide, *J. Am. Chem. Soc.*, 1951, **73**, p 3894-3895
14. J.L. Shapiro, B.F. Woodfield, R. Stevens, J. Boerio-Goates, and M.L. Wilson, Molar Heat Capacity and Thermodynamic Functions of the Type II Antiferromagnet MnO, *J. Chem. Thermodyn.*, 1999, **31**, p 725-739
15. R. Georges, E. Gmelin, D. Landau, and J. Lasjaunias, Specific Heat at Low Temperature of Manganese Sulphide and Oxide, *C.R. Acad. Sc. Paris*, 1969, **269**, p 827-830
16. J.C. Southard and C.H. Shomate, Heat of Formation and High-Temperature Heat Content of Manganous Oxide and Manganous Sulphate. High-Temperature Heat Content of Manganese, *J. Am. Chem. Soc.*, 1942, **64**, p 1770-1774
17. P.D. Desai, Thermodynamic Properties of Manganese and Molybdenum, *J. Phys. Chem. Ref. Data*, 1987, **16**, p 91-108
18. M.W. Chase, Jr., C.A. Davies, J.R. Downey, Jr., D.J. Frurip, R.A. McDonald, and A.N. Syverud, JANAF Thermochemical Tables, 3rd ed., Part II, *J. Phys. Chem. Ref. Data*, **14**(Suppl. 1), 1985, p 1667
19. H. Siemonsen, A New Determination of the Heat of Formation of the Oxides of Manganese, *Zeit. Elektrochem. Angew. Physikal. Chemie*, 1939, **45**, p 637-643
20. R.A. Robie and B.S. Hemingway, Low-Temperature Molar Heat Capacity and Entropies of MnO_2 (Pyrolusite), Mn_3O_4

(Hausmanite) and Mn_2O_3 (bixbyite), *J. Am. Chem. Soc.*, 1985, **17**, p 165-181
21. D.D. Wagman, W.H. Evans, V.B. Parker, I. Halow, S.M. Bailey, R.H. Schumm, and K.L. Churney, "Selected Values of Chemical Thermodynamic Properties, Tables for Elements 35 Through 53 in the Standard Order of Arrangement," NBS Tech. Note 270-4, 1969, p 106
22. O. Knacke, O. Kubaschewski, and K. Hesselman, *Thermodynamic Properties of Inorganic Substances*. Springer-Verlag, Berlin, Germany, 1991, p 1182-1185